
Research Article: New Research | Cognition and Behavior

Facilitated Event-Related Power-Modulations during Transcranial Alternating Current Stimulation (tACS) Revealed by Concurrent tACS-MEG

Florian H. Kasten^{1,2}, Burkhard Maess³ and Christoph S. Herrmann^{1,2,4}

¹*Experimental Psychology Lab, Department of Psychology, European Medical School, Cluster for Excellence "Hearing for All", Carl Von Ossietzky University, Oldenburg, Germany*

²*Neuroimaging Unit, European Medical School, Carl Von Ossietzky University, Oldenburg, Germany*

³*MEG and Cortical Networks Group, Max Planck Institute for Human Cognitive and Brain Sciences, Leipzig, Germany*

⁴*Research Center Neurosensory Science, Carl Von Ossietzky University, Oldenburg, Germany*

DOI: 10.1523/ENEURO.0069-18.2018

Received: 13 February 2018

Revised: 1 June 2018

Accepted: 7 June 2018

Published: 25 June 2018

Author contributions: FHK, BM and CSH conceived the study and wrote the manuscript. FHK and BM collected the data. FHK analyzed the data. BM and CSH provided equipment and funding for the study.

Funding: <http://doi.org/10.13039/501100001659> Deutsche Forschungsgemeinschaft (DFG)
DFG
SPP
1665 HE 3353/8-2

CSH holds a patent on brain stimulation and received honoraria as editor from Elsevier Publishers, Amsterdam. FHK and BM declare no competing interests.

This research was supported by a grant of the German Research Foundation (Deutsche Forschungsgemeinschaft, DFG) awarded to Christoph S. Herrmann (DFG, SPP, 1665 HE 3353/8-2).

Corresponding author: Christoph S. Herrmann, Experimental Psychology Lab, Carl von Ossietzky University, Ammerländer Heerstr. 114 – 118, 26129, Oldenburg, Germany. Tel: +49 441 798 4936; E-mail: christoph.herrmann@uni-oldenburg.de

Cite as: eNeuro 2018; 10.1523/ENEURO.0069-18.2018

Alerts: Sign up at eneuro.org/alerts to receive customized email alerts when the fully formatted version of this article is published.

Accepted manuscripts are peer-reviewed but have not been through the copyediting, formatting, or proofreading process.

Copyright © 2018 Kasten et al.

This is an open-access article distributed under the terms of the Creative Commons Attribution 4.0 International license, which permits unrestricted use, distribution and reproduction in any medium provided that the original work is properly attributed.

1 **Facilitated event-related power-modulations during transcranial**
2 **alternating current stimulation (tACS) revealed by concurrent**
3 **tACS-MEG**

4 **Abbreviated title:** Facilitated event-related power-modulations during
5 tACS

6 Florian H. Kasten^{1,2}, Burkhard Maess³, Christoph S. Herrmann^{1,2,4,*}

7 ¹Experimental Psychology Lab, Department of Psychology, European Medical School, Cluster for Ex-
8 cellence "Hearing for All", Carl von Ossietzky University, Oldenburg, Germany

9 ²Neuroimaging Unit, European Medical School, Carl von Ossietzky University, Oldenburg, Germany

10 ³MEG and Cortical Networks Group, Max Planck Institute for Human Cognitive and Brain Sciences,
11 Leipzig, Germany

12 ⁴Research Center Neurosensory Science, Carl von Ossietzky University, Oldenburg, Germany

13 *Corresponding author:

14 Christoph S. Herrmann,

15 Experimental Psychology Lab, Carl von Ossietzky University,

16 Ammerländer Heerstr. 114 – 118,

17 26129, Oldenburg, Germany.

18 christoph.herrmann@uni-oldenburg.de, phone: +49 441 798 4936

19

20 Number of words: Abstract (244), Significance (113), Introduction (749), Discussion (1951)

21 Number of pages: 34

22 Number of Figures: 6

23 **Conflict of interest:** CSH holds a patent on brain stimulation and received honoraria as editor
24 from Elsevier Publishers, Amsterdam. FHK and BM declare no competing interests.

25

26 **Keywords:** transcranial alternating current stimulation (tACS), MEG, online effects, event-re-
27 lated oscillations, cognitive performance

28

29 **Acknowledgements:**

30 The authors would like to thank Yvonne Wolf-Rosier for her invaluable efforts and assistance
31 during data collection and Dr. Joshua Grant for proofreading the manuscript.

32 This research was supported by a grant of the German Research Foundation (Deutsche For-
33 schungsgemeinschaft, DFG) awarded to Christoph S. Herrmann (DFG, SPP, 1665 HE 3353/8-
34 2).

35

36 **Abstract**

37 Non-invasive approaches to modulate oscillatory activity in the brain are increasingly popular
38 in the scientific community. Transcranial alternating current stimulation (tACS) has been shown
39 to modulate neural oscillations in a frequency specific manner. However, due to a massive
40 stimulation artifact at the targeted frequency, little is known about effects of tACS during stim-
41 ulation. It remains unclear how the continuous application of tACS affects event-related oscil-
42 lations during cognitive tasks. Depending on whether tACS influences pre- or post-stimulus
43 oscillations, or both, the endogenous, event-related oscillatory dynamics could be pushed in
44 various directions or not at all. A better understanding of these effects is crucial to plan, predict
45 and understand outcomes of solely behavioral tACS experiments. In the present study, a re-
46 cently proposed procedure to suppress tACS artifacts by projecting MEG data into source-
47 space using spatial filtering was utilized to recover event-related power modulations in the
48 alpha-band during a mental rotation task. MEG data of twenty-five human subjects was con-
49 tinuously recorded. After 10 a minute baseline measurement, participants received either 20
50 minutes of tACS at their individual alpha frequency, or sham stimulation. Another 40 minutes
51 of MEG data were acquired thereafter. Data were projected into source-space and carefully
52 examined for residual artifacts. Results revealed strong facilitation of event-related power mod-
53 ulations in the alpha-band during tACS application. These results provide first direct evidence,
54 that tACS does not counteract top-down suppression of intrinsic oscillations, but rather en-
55 hances pre-existent power modulations within the range of the individual alpha (=stimulation)
56 frequency.

57 **Significance**

58 Transcranial alternating current stimulation (tACS) is increasingly used in cognitive neurosci-
59 ence to study the causal role of brain oscillations for cognition. However, online effects of tACS
60 largely remain a 'black box' due to an intense electromagnetic artifact encountered during
61 stimulation. The current study is the first to employ a spatial filtering approach to recover, and
62 systematically study, event-related oscillatory dynamics during tACS, which could potentially
63 be altered in various directions. TACS facilitated pre-existing patterns of oscillatory dynamics
64 during the employed mental rotation task, but did not counteract or overwrite them. In addition,
65 control analyses and a measure to quantify tACS artifact suppression are provided that can
66 enrich future studies investigating tACS online effects.

67 **1 Introduction**

68 Oscillatory activity of neuronal assemblies is a ubiquitous phenomenon in the brain observed
69 within and between different brain structures and across species (Buzsáki, 2006). Over the
70 past decades these oscillations have been linked to a variety of brain functions, such as
71 memory, perception, and cognitive performance (Klimesch, 1999; Basar et al., 2000; Buzsáki,
72 2006; Klimesch et al., 2007). Traditionally, these relationships were fruitfully investigated using
73 imaging techniques such as electro- or magnetoencephalography (EEG/MEG). However, in
74 their nature these approaches are correlational and cannot resolve causal relationships be-
75 tween neural oscillations and cognitive processes. The recent (re-)discovery of non-invasive
76 transcranial electrical stimulation (tES) now allows to directly probe these causal relationships
77 (Herrmann et al., 2016b).

78 The application of oscillatory currents through the scalp by means of transcranial alternating
79 current stimulation (tACS), has been shown to modulate endogenous brain oscillations in a
80 frequency specific manner (Fröhlich and McCormick, 2010; Ozen et al., 2010; Zaehle et al.,
81 2010; Helfrich et al., 2014). Effects of tACS during stimulation have been primarily investigated
82 in animals (Fröhlich and McCormick, 2010; Ozen et al., 2010; Kar et al., 2017) and with com-
83 putational models (Fröhlich and McCormick, 2010; Reato et al., 2010; Ali et al., 2013;
84 Negahbani et al., 2018). Due to a massive artifact introduced to electrophysiological signals,
85 studies on tACS effects in humans have mostly been restricted to behavioral measures
86 (Marshall et al., 2006; Kar and Kregelberg, 2014; Lustenberger et al., 2015), BOLD-signal
87 effects (Alekseichuk et al., 2016; Cabral-Calderin et al., 2016; Vosskuhl et al., 2016; Violante
88 et al., 2017) and aftereffects in M/EEG (Zaehle et al., 2010; Wach et al., 2013; Neuling et al.,
89 2015; Veniero et al., 2015; Vossen et al., 2015; Kasten et al., 2016; Stecher et al., 2017). In
90 case of M/EEG, a frequency specific increase in oscillatory power after stimulation is consist-
91 ently reported (Zaehle et al., 2010; Neuling et al., 2013; Vossen et al., 2015; Kasten et al.,
92 2016). It is often assumed that the underlying mechanism of action of tACS is entrainment of
93 neural activity to the external driving force, which is observed in computational and animal
94 models (Fröhlich and McCormick, 2010; Ozen et al., 2010; Reato et al., 2010; Ali et al., 2013;

95 Negahbani et al., 2018). Direct evidence for entrainment of brain oscillations to tACS in hu-
96 mans is, however, largely missing so far.

97 Besides sustained effects on the power of spontaneous oscillations after the stimulation, tACS
98 has more recently been demonstrated to alter event-related oscillatory dynamics in the context
99 of a cognitive task (Kasten and Herrmann, 2017). In that study, event-related desynchroniza-
100 tion (ERD) was enhanced after tACS application, accompanied by improved performance in a
101 classic mental rotation (MR) task (Shepard and Metzler, 1971; Kasten and Herrmann, 2017).
102 The amount of ERD in the alpha-band has previously been linked to MR performance (Michel
103 et al., 1994; Klimesch et al., 2003). Although an increase in task performance has already been
104 observed during tACS, the precise oscillatory dynamics during tACS remain unclear (Kasten
105 and Herrmann, 2017). Given that many tACS-studies rely solely on behavioral measures, an
106 understanding of the effect of tACS on event-related oscillations is crucial. Depending on
107 whether the stimulation merely affects pre- or post-stimulus oscillations or both, tACS may
108 increase, decrease or not modulate ERD/ERS. Each of these scenarios would result in differ-
109 ent behavioral outcomes to be expected. The current study aims to provide a first step towards
110 understanding the effects of tACS on event-related power-modulations *during* stimulation. To
111 this end, the experiment of Kasten and Herrmann (2017) was repeated in an MEG scanner.
112 The application of linearly constrained minimum variance beamforming (LCMV, Van Veen et
113 al., 1997) on MEG recordings has been shown to substantially suppress electromagnetic arti-
114 facts encountered during tES (Soekadar et al., 2013; Neuling et al., 2015). Although this ap-
115 proach will never completely remove artifacts from the signal (Noury et al., 2016; Mäkelä et
116 al., 2017; Noury and Siegel, 2017), artifact suppression may still be sufficient to recover
117 changes in event-related dynamics during tACS (Neuling et al., 2017; Noury and Siegel, 2018).
118 In the present study, LCMV was utilized to attempt to recover the event-related power-modu-
119 lations in the alpha-band encountered during MR. Based on previous behavioral results, an
120 increase in alpha-power modulation during tACS was hypothesized (Kasten and Herrmann,
121 2017). The measure to capture tACS effects (absolute power difference instead of relative
122 change) was carefully chosen to be robust against the possible influence of residual artifacts.

123 Careful control analyses were conducted to rule out that the observed effects can be attributed
124 to a residual artifact.

125 **2 Methods**

126 **2.1 Participants**

127 Twenty-five healthy volunteers were randomly assigned to one of two experimental conditions.
128 They received either 20 minutes of tACS or sham stimulation during the course of the experi-
129 ment. All were right-handed according to the Edinburgh Handedness Inventory (Oldfield, 1971)
130 and had normal or corrected to normal vision. Participants gave written informed consent prior
131 to the experiment and reported no history of neurological or psychiatric conditions. The exper-
132 iment was approved by the “*Commission for Research Impact Assessment and Ethics*” at the
133 University of Oldenburg and conducted in accordance with the declaration of Helsinki. Three
134 subjects exhibited low tolerance to skin or phosphene sensations while determining the indi-
135 vidual stimulation intensity (see section 2.3). Due to the resulting low stimulation currents (be-
136 low 0.4 mA) these subjects were excluded from the analysis. Furthermore, two participants
137 were excluded as they did not exhibit alpha modulation in response to the cognitive task during
138 the baseline block. Data of twenty subjects (10 in stimulation group, 10 in sham group, age:
139 26 ± 3 years, 8 females) remained for analysis. Although the groups were initially counterbal-
140 anced for participants’ sex, the exclusion of subjects resulted in an imbalance in the sham
141 group (7 males vs. 3 females, 5 males vs. 5 females in the stimulation group).

142 **2.2 Magnetoencephalogram**

143 Neuromagnetic activity was recorded at a rate of 1 kHz using a 306 channel whole-head MEG
144 system (Elekta Neuromag Vectorview, Elekta Oy, Helsinki, Finland) with 102 magnetometers
145 and 204 orthogonal, planar gradiometers, sampling from 102 distinct sensor locations. An
146 online band-pass filter between 0.1 Hz and 330 Hz was applied. The experiment was con-
147 ducted in a dimly lit, magnetically shielded room (MSR; Vacuumschmelze, Hanau, Germany)
148 with participants seated below the MEG helmet in upright position. Prior to the experiment,
149 three anatomical landmarks (nasion, left and right posterior tip of tragi) were digitized using a

150 Polhemus Fastrack (Polhemus, Colchester, VT, USA), along with the location of five head
151 position indicator (HPI) coils, and > 200 head shape samples to allow continuous head-position
152 tracking and later co-registration with anatomical MRIs.

153 After finishing the preparations, individual alpha frequency (IAF) was determined from a three-
154 minute, eyes-open, resting-state MEG recording. Data were segmented into 1 s epochs. Fast
155 Fourier Transforms (FFTs) were computed for each of the segments using the Fieldtrip toolbox
156 (Oostenveld et al., 2011). The power peak in the averaged spectra, in the 8-12 Hz band, was
157 determined in a set of posterior sensors showing most pronounced alpha activity by visual
158 inspection. The identified frequency was used as stimulation frequency for the subsequent
159 procedures (refer to **Figure 1A** for an overview of the time course of the experiment and **Figure**
160 **1B** for an illustration of sensor locations used to determine participants' IAF).

161 **2.3 Electrical stimulation**

162 Participants received either 20 minutes of tACS (including 10 s fade-in and fade-out) or sham
163 stimulation (30 s stimulation in the beginning of the stimulation period, including 10 s fade-in
164 and out) at their individual alpha frequency (IAF). The sinusoidal stimulation signal was digitally
165 generated at a sampling rate of 10 kHz in Matlab 2012a (32-bit, The MathWorks Inc., Natick,
166 MA, USA) and transferred to a digital-analog converter (Ni USB 6221, National Instruments,
167 Austin, TX, USA). From there the signal was streamed to the remote input of a battery-driven
168 constant current stimulator (DC Stimulator Plus, Neuroconn, Illmenau, Germany), which was
169 placed inside an electrically shielded cabinet outside the MSR. The signal was then gated into
170 the MSR via a tube in the wall using the MRI extension-kit of the stimulator (Neuroconn, Ill-
171 menau, Germany). Electrical Stimulation was administered by two surface conductive rubber
172 electrodes attached to participants scalp over electrode positions Cz (5 x 7 cm) and Oz (4 x 4
173 cm) of the international 10-10 system (**Figure 1B**), using an adhesive, electrically conductive
174 paste (ten20 Conductive Paste, Weaver and Co., USA). Impedance was kept below 20 k Ω
175 (including two 5 k Ω resistors in the cables of the MRI extension-kit of the stimulator). Accord-
176 ingly, impedance between the electrodes was limited to 10 k Ω .

177 To minimize confounding influences from either phosphene or skin sensations, tACS was ap-
178 plied below participants' individual sensation threshold, using an established thresholding pro-
179 cedure (Neuling et al., 2013, 2015; Kasten et al., 2016; Kasten and Herrmann, 2017). To this
180 end, participants were stimulated with an initial intensity of 500 μ A at their IAF. Depending on
181 whether participants noticed the initial stimulation, intensity was either increased or decreased
182 in steps of 100 μ A until they noticed/not noticed the stimulation. The highest intensity at which
183 participants did not notice the stimulation was subsequently used as tACS intensity in the main
184 experiment. The thresholding was performed for both groups in order to keep experimental
185 procedures similar. The obtained intensities for the sham group were applied during the 30 s
186 stimulation train in the beginning of the stimulation block (see above). Three participants ex-
187 hibited sensation thresholds below 400 μ A and were excluded from analysis. On average,
188 participants were stimulated with 715 μ A \pm 301 μ A (peak-to-peak; stimulation group: 680 μ A \pm
189 175 μ A) at a frequency of 10.5 Hz \pm 0.9 Hz. TACS or sham stimulation was applied, immedi-
190 ately following the baseline block, for 20 minutes during the second and third block of the
191 behavioral experiment.

192 **2.4 Mental rotation task**

193 Visual stimuli were presented using Psychtoolbox 3 (Kleiner et al., 2007) implemented in the
194 same Matlab script that generated the electrical stimulation signal. Visual stimuli were rear-
195 projected onto a screen inside the MSR at a distance of \sim 100 cm from the participant.

196 Subjects performed the same MR paradigm that was employed in a recent tACS-EEG study
197 (Kasten and Herrmann, 2017). Stimuli were taken from an open-source stimulus set (Ganis
198 and Kievit, 2015), comprised of 384 MR stimuli (pairs of 2 dimensional objects) similar to the
199 objects used in the seminal paper of Shepard and Metzler (1971). The duration of the experi-
200 ment was reduced from 8 to 7 blocks of 10 minutes each. Participants were familiarized with
201 the task on a laptop during electrode preparation (16 practice trials with immediate feedback).
202 All other parameters were kept similar. Each block consisted of 48 trials, starting with the
203 presentation of a white fixation cross at the center of the screen. After 3000 ms a MR stimulus
204 was presented for 7000 ms. During this time participants were asked to judge whether the two

205 objects on the screen were either identical (can be brought into alignment by rotating) or dif-
206 ferent (cannot be brought into alignment by rotating) by pressing a button with their left or right
207 index finger (**Figure 1C**). To keep visual stimulation at a constant level, the MR stimuli re-
208 mained on screen for the whole 7000 ms, regardless of participants' reaction times. Every 24
209 trials, the task was interrupted by a one minute resting period during which a rotation of the
210 fixation cross had to be detected. This ensured that participants remained focused and tried to
211 avoid head movements. The first block served as a baseline measurement before stimulation.
212 During the second and third block, tACS or sham stimulation was applied. The remaining four
213 blocks served as post-stimulation measurements to capture aftereffects of the stimulation (**Fig-**
214 **ure 1A**). The experiment had a total duration of 70 minutes.

215 **2.5 Debriefing**

216 After finishing the experiment, participants filled out a translated version of a questionnaire
217 assessing commonly reported side effects of transcranial electrical stimulation (Brunoni et al.,
218 2011). Subsequently, they were asked to indicate whether they believe they received tACS or
219 sham stimulation. Finally, all subjects were informed about the aims of the experiment and
220 their actual experimental condition.

221 **2.6 Data analysis**

222 Data analysis was performed using Matlab 2016a (The MathWorks Inc., Natick, MA, USA).
223 MEG data processing was performed using the Fieldtrip toolbox (Oostenveld et al., 2011) em-
224 bedded in custom Matlab scripts.

225 **2.6.1 Behavioral data**

226 Analysis of performance and reaction time (RT) data followed the approach of Kasten and
227 Herrmann (2017). Performance, in percentage correct, in each block (48 Trials) was calculated
228 and normalized by pre-stimulation baseline to account for inter-individual differences. The re-
229 sulting values reflect performance change in each block relative to baseline. RTs were aver-
230 aged separately for each rotation angle and normalized by their respective baseline RT. The

231 normalized RTs were then averaged over angles for each block. This procedure accounts for
232 the known increase in RT with larger rotation angles (Shepard and Metzler, 1971).

233 **2.6.2 MEG processing and artifact suppression**

234 MEG data were resampled to 250 Hz and filtered between 1 and 40 Hz using a 4th order, zero-
235 phase Butterworth filter. Data were projected into source-space by application of a linearly
236 constrained minimum variance (LCMV) beamformer (Van Veen et al., 1997), a procedure that
237 has been demonstrated to suppress artifacts originating from transcranial electrical stimulation
238 (Soekadar et al., 2013; Neuling et al., 2015). Filter coefficients were individually estimated for
239 each block using the noise covariance matrix, an equally spaced (1.5 cm) 889 point grid
240 warped into Montreal Neurological Institute (MNI) space, and single-shell headmodels (Nolte,
241 2003), created from individual T1-weighted MRIs. MRIs were co-registered to the median head
242 position in each block, estimated from continuous HPI signals using the Elekta Neuromag
243 MaxFilter™ software (Elekta Oy, Helsinki, Finland). The signal-space-separation method
244 (Taulu et al., 2005), offered by the software was not applied, as it seemed to corrupt tACS
245 artefact suppression after beamforming. Covariance matrices were estimated by segmenting
246 each MEG recording into 2 s epochs. The regularization parameter λ for the LCMV beamformer
247 was set to zero to ensure optimal artifact suppression as suggested by Neuling et al. (2017).
248 Sensor-space MEG data were segmented -5 s to 7 s around the onset of the MR stimuli.
249 Epochs were then projected into source-space using the previously obtained beamformer fil-
250 ters, resulting in 889 virtual channels, distributed over the brain. A time-frequency analysis was
251 computed for all trials using Morlet-wavelets with a fixed width of 7 cycles. The resulting time-
252 frequency spectra were subsequently averaged for each block.

253 As mentioned above, all analysis procedures in this study were rigorously checked with respect
254 to their robustness against the influence of residual artifacts in the data (Noury et al., 2016;
255 Neuling et al., 2017). This involved a careful choice of the measure used to capture event-
256 related changes in oscillatory power. Traditionally, such changes have been evaluated using
257 the concept of event-related (de-)synchronization (ERD/ERS), which has been defined by
258 Pfurtscheller and Lopes Da Silva (1999) as:

$$ERD/ERS = \frac{R-A}{R} * 100, \quad (1)$$

where R is the oscillatory power within the frequency band of interest during a reference period, prior to stimulus onset, and A is the power during a testing period after stimulus onset, respectively. However, assuming that residual tACS artifacts (R_{Res} and A_{Res}) are equally contributing to R and A , this would change the equation in the following way:

$$ERD/ERS = \frac{(R+R_{Res})-(A+A_{Res})}{(R+R_{Res})} * 100 \quad (2)$$

Given that the residuals in R and A are uncorrelated with the task and have approximately equal strength ($R_{Res} \approx A_{Res}$), their influence cancels out in the numerator, but biases the denominator of the equation, resulting in systematic underestimations of the observed power modulations:

$$ERD/ERS = \frac{R-A}{(R+R_{Res})} * 100 \quad (3)$$

For this reason the pure difference between reference and testing period (for the sake of clarity referred to as event-related power difference; $ER\Delta_{Pow}$) was used to more accurately capture event-related power modulations in the current study:

$$ER\Delta_{Pow} = (R + R_{Res}) - (A + A_{Res}) = R - A \quad (4)$$

Power in the individual alpha-band (IAF \pm 2 Hz) was extracted with the reference and test periods ranging from -2.5 s to -0.5 before and 0 s to 2 s after stimulus onset, respectively.

Performance of the artifact suppression was evaluated by estimating the size of the residual artifact relative to the brain oscillation of interest (see next section). As will be described in more detail in the results section, the beamformer successfully suppressed the tACS artifact from ~2,500,000 times the size of human alpha oscillations down to a factor of < 3 . However, some 'hot spots', showing larger residual artifacts (1:10), are apparent in the proximity of stimulator cables and the central stimulation electrode. In order to avoid the inclusion of virtual channels in the analysis, that contain strong residual artifacts, but no physiologically meaningful effects, brain areas showing strongest alpha-power modulation in response to the onset of the MR-stimuli were localized based on the first (artifact-free) block prior to stimulation. To this

285 end, a dependent-sample random permutation cluster t-test (two-tailed) with 5000 randomiza-
286 tions and Monte Carlo estimates to calculate p -values, was run to compare power in the IAF-
287 band between the reference and test periods during the baseline block. The test was per-
288 formed on the whole sample (stimulation and sham group pooled). Clusters were thresholded
289 at an α -level of .01. The resulting significant negative cluster was used as a ROI to extract the
290 time course of $ER\Delta_{Pow}$ from each block. To account for inter-individual differences, $ER\Delta_{Pow}$ in
291 each block was normalized by $ER\Delta_{Pow}$ in the baseline block before stimulation. In order to test
292 whether the effects of tACS were specific to the alpha-band, the same analysis was performed
293 on power modulations in the lower (IAF + 3 Hz to IAF + 11 Hz) and upper (IAF + 12 Hz to IAF
294 + 20 Hz) beta-bands within the ROI.

295 **2.6.3 Evaluation of artifact suppression and control analyses**

296 As discussed earlier, the application of LCMV beamforming results in a strong, yet imperfect
297 suppression of the tACS artifact (Noury et al., 2016; Mäkelä et al., 2017; Noury and Siegel,
298 2017). It is therefore crucial to characterize the achieved artifact suppression and to rule out
299 the possibility that the effects observed during stimulation result from residual artifacts in the
300 data, rather than a true effect of tACS on the brain.

301 In order to evaluate the artifact suppression achieved by the spatial filtering procedure, partic-
302 ipants' alpha-power (IAF \pm 2 Hz) was extracted from the pre-stimulus interval of the baseline
303 and the two stimulation blocks. The power in the baseline block provides an estimate of par-
304 ticipants' natural, artifact-free alpha-power, that can be compared to the power encountered
305 during stimulation blocks before (on the sensor-level) and after beamforming (on the source-
306 level). It is therefore possible to roughly estimate the size of the stimulation artifact relative to
307 the brain signal of interest. This artifact-to-brain-signal-ratio was calculated for each magneto-
308 and gradiometer channel as well as for each virtual channel after LCMV. While this measure
309 is not able to disentangle brain signal/tACS effects from a residual artifact after LCMV, it can
310 provide an upper boundary for the size of the residual artifact and allows the inspection of its
311 spatial distribution.

312 A major assumption of the presented analysis framework, for event-related power modulations
313 during tACS, is that the (residual) artifact has similar strength during the pre- and post-stimulus
314 intervals, such that its influence cancels out when contrasting (subtracting) the two intervals
315 (**Equation 4**). Previous studies have demonstrated that physiological processes such as heart-
316 beat and respiration can result in impedance changes of body tissue and small body move-
317 ments, which change the size of the tACS artifact (Noury et al., 2016; Noury and Siegel, 2017).
318 To rule out a similar modulation of artifact strength, occurring in an event-related manner, ac-
319 counting for potential effects observed on the source-level, a control analysis was carried out.
320 Sensor-level MEG time-series during the two stimulation blocks were band-pass filtered
321 around the stimulation frequency ($IAF \pm 1$ Hz) and the signal envelope was extracted using a
322 Hilbert transform. The envelope time-series was subsequently segmented analogously to the
323 $ER\Delta_{Pow}$ analysis and demeaned. The difference in envelope amplitude during pre- (-2.5s to -
324 0.5s) and post-stimulus interval (0 – 2 s) were compared by means of a random permutation
325 cluster t-test with Monte Carlo estimates. To rule out the possibility that these differences drive
326 the effects observed on the source-level, the envelope differences were correlated with the
327 $ER\Delta_{Pow}$ values obtained earlier. For comparison, the same analysis was performed for the
328 stimulation and sham group. For the sham group, envelope differences should reflect the
329 event-related suppression of alpha-power, commonly observed during MR, and therefore
330 highly correlate with the source-level $ER\Delta_{Pow}$. Pre- vs. post-stimulus envelope differences in
331 the stimulation group, however, should pre-dominantly reflect changes in the tACS artifact.
332 High correlations between sensor-space envelope differences and source-level $ER\Delta_{Pow}$ would
333 thus indicate that systematic modulations of the tACS artifact drive changes in $ER\Delta_{Pow}$, rather
334 than an actual physiological effect of tACS.

335 **2.6.4 Experimental design and statistical analysis**

336 Statistical analysis was realized in a 2 x 6 mixed-effects repeated measures design with the
337 between subject factor *condition* (stimulation vs. sham) and the within subject factor *block* (6
338 levels). The normalized behavioral (performance, RTs) and physiological ($ER\Delta_{Pow}$) data were
339 analyzed using repeated measures ANOVAs (rmANOVA). Greenhouse-Geisser corrected p-

340 values are reported were appropriate. If significant interactions between *condition* and *block*
341 were revealed, analysis was subsequently split into two separate rmANOVAs, one covering
342 the effects during stimulation (factors condition: stimulation vs. sham; block: block 2 vs. block
343 3) and the other analyzing outlasting effects (factors condition: stimulation vs. sham; block:
344 block 4 -block 7). Comparisons of single blocks were performed using two-sample t-tests. Gen-
345 eralized η^2 and *Cohen's d* values are reported as measures of effect size. Pearson's correlation
346 coefficients were calculated to relate behavioral and physiological effects, as well as physio-
347 logical effects and stimulation intensity.

348 Statistical analysis was performed using R 3.2.3 (The R Core Team, R Foundation for Statis-
349 tical Computing, Vienna, Austria). Cluster based permutation tests on MEG data were per-
350 formed in Matlab 2016a using statistical functions implemented in the Fieldtrip toolbox
351 (Oostenveld et al., 2011).

352 2.6.5 Code accessibility

353 All scripts underlying the presented results are available as "*Extended Data*" and can be ac-
354 cessed online via the open science framework: <https://osf.io/btnu7/>.

355 3 Results

356 3.1 Behavioral results

357 A Welch's two sample t-test yielded a trend for slightly better raw task performance in the
358 baseline block for the sham group as compared to the stimulation group ($t_{14.9} = -2.00$, $p = .06$,
359 $d = .9$; $M_{stim} = 87.3\%$, $SD = 3.6\%$; $M_{Sham} = 91.7\%$, $SD = 5.9\%$). The rmANOVA on relative
360 performance change revealed a significantly larger facilitation of MR performance, relative to
361 baseline, in the *stimulation* group as compared to *sham* (condition: $F_{1,18} = 4.93$, $p = .04$, $\eta^2 =$
362 0.14). Average performance during and after stimulation was $M_{Stim} = 92.3\%$ ($SD = 2.5\%$) and
363 $M_{Sham} = 90.9\%$ ($SD = 5.6\%$), respectively.

364 Experimental groups did not differ with respect to their baseline RTs ($t_{16} = 0.3$, $p = .77$, $d = .13$,
365 $M_{Stim} = 2763$ ms, $SD = 848$ ms, $M_{Sham} = 2660$ ms, $SD = 659$ ms). Analysis of the normalized
366 RTs revealed a trend for the factor *block* ($F_{5,90} = 2.47$, $p = .07$, $\eta^2 = 0.03$), but no effect of

367 stimulation ($F_{1,18} = 1.02$, $p = .33$, $\eta^2 = 0.04$). Mean reaction times during and after stimulation
368 were $M_{Stim} = 2597$ ms ($SD = 710$ ms) and $M_{Sham} = 2371$ ms ($SD = 524$ ms) on average. Results
369 of the behavioral analysis are summarized in **Figure 2**.

370 **3.2 Event-related alpha modulation**

371 Comparison of pre- and post-stimulus IAF-band power, during the baseline block, revealed a
372 significant cluster in occipito-parietal areas ($p_{cluster} < .001$, **Figure 3A**) for the whole sample.
373 The identified cluster was used as a ROI to extract the time-course of $ER\Delta_{Pow}$ from the different
374 blocks and to limit the subsequent analysis to physiologically meaningful brain regions. The
375 subsequent rmANOVA revealed a significant main effect of *block* ($F_{5,90} = 7.22$, $p = .009$, $\eta^2 =$
376 $.15$) as well as a significant *condition*block* interaction ($F_{5,90} = 6.81$, $p = .011$, $\eta^2 = .15$), and a
377 trend for the main effect of *condition* ($F_{1,18} = 3.62$, $p = .07$, $\eta^2 = .10$). Please refer to **Figure 3B**
378 for an overview of the time-course of relative $ER\Delta_{Pow}$. To further resolve the significant inter-
379 action, separate rmANOVAs were performed on the data acquired during and after tACS.
380 These analyses exhibited a significant main effect of *condition* ($F_{1,18} = 9.34$, $p = .007$, $\eta^2 = .27$)
381 during stimulation, but not thereafter (*condition*: $F_{1,18} = 0.14$, $p = .71$, $\eta^2 < .01$, **Figure 3C**).
382 Furthermore, a significant effect of *block* ($F_{3,54} = 3.55$, $p = .02$, $\eta^2 = .02$), as well as a significant
383 *condition*block* interaction ($F_{3,54} = 3.10$, $p = .034$, $\eta^2 = .02$) were found in the post-stimulation
384 data. None of the other main effects or interactions reached significance. It was not possible
385 to further resolve the significant *condition*block* interaction during the post-stimulation blocks.
386 Separately testing relative $ER\Delta_{Pow}$ values of the two experimental groups against each other
387 did not reveal significant differences for any of the blocks (all $p > .12$, Welch two-sample t-test,
388 one-tailed, uncorrected). Based on pure visual inspection, the interaction appears to be driven
389 by a group difference during the first block after stimulation (block 4, see **Figure 3B**), which
390 might be indicative of a weak tACS aftereffect during this block. Refer to **Figure 4** for group-
391 averaged time-frequency representations of participants' normalized alpha-power change and
392 the corresponding source-level topographies within the analyzed ROI.
393 No significant correlation between the increase in $ER\Delta_{Pow}$ during stimulation and stimulation
394 intensity was observed in the *stimulation* group ($r = .40$, $t_8 = 1.25$, $p = .24$). A weak, negative,

395 non-significant correlation was observed in the *sham* group ($r = -.26$, $t_8 = -0.78$, $p = .45$; **Figure**
396 **3D**).

397 To test whether the effects of tACS were specific to the alpha-band, the analysis was repeated
398 on event-related power modulations in the lower (IAF + 3 Hz to IAF + 11 Hz) and upper (IAF +
399 12 Hz to IAF + 20 Hz) beta-bands within the ROI. The rmANOVA for the lower beta-band
400 revealed a significant effect of *block* ($F_{5,90} = 15.10$, $p < .001$, $\eta^2 = .17$) as well as a significant
401 *condition*block* interaction ($F_{5,90} = 9.37$, $p < .001$, $\eta^2 = .11$). Two separate rmANOVAs, testing
402 the effects during and after stimulation, revealed a trend for the factor *condition* during stimu-
403 lation ($F_{1,18} = 4.17$, $p = .056$, $\eta^2 = .18$) as well as a significant effect of *block* ($F_{1,18} = 4.72$, $p =$
404 $.043$, $\eta^2 = .02$). After stimulation, only a trend for the factor *block* was found ($F_{3,54} = 2.28$, $p =$
405 $.09$, $\eta^2 = .03$). No significant effects were found in the analysis of the upper beta-band. **Figure**
406 **3E,F** summarize results for the lower and upper beta-band analysis (all $p > .1$).

407 There were no significant correlations between relative $ER\Delta_{Pow}$ and change in task perfor-
408 mance during ($r_{online} = .3$, $t_{18} = 1.37$, $p = .18$) or after stimulation ($r_{offline} = .11$, $t_{18} = 0.49$, $p = .62$).
409 Descriptively, the correlation was higher for the sham group both during and after stimulation
410 ($r_{Sham/online} = .51$, $t_8 = 1.67$, $p = .13$; $r_{Sham/offline} = .54$, $t_8 = 1.83$, $p = .1$) as compared to the stimu-
411 lation group ($r_{Stim/online} = .09$, $t_8 = 0.27$, $p = .8$; $r_{Stim/offline} = -.16$, $t_8 = -0.45$, $p = .67$; **Figure 3G,H**).

412 **3.3 Control analyses**

413 To rule out the possibility that the strikingly strong facilitation of power-modulation in the alpha-
414 band was driven by residual artifacts, several control analyses were performed. In a first step,
415 the performance of the artifact suppression achieved by LCMV was evaluated. To this end, the
416 ratio of pre-stimulus alpha-power during the (tACS-free) baseline block and the two tACS
417 blocks was compared in sensor- and source-space. On average, this artifact-to-brain-signal-
418 ratio was 2,534,000:1 in block 2 and 2,569,000:1 in block 3 (average over all sensors and
419 subjects) in the sensor-space data. After LCMV beamforming the ratio was reduced to 2.72:1
420 in block 2 and 3.13:1 in block 3 (average over virtual sensors and subjects). The largest ratio
421 observed in a single virtual channel of one subject after beamforming was 93.42:1. **Figure 5**
422 illustrates the spatial distribution of the artifact-to-brain-signal-ratio on the source-level. The

423 ratio was highest in central areas, covered by stimulation electrodes and cables. Outside of
424 these areas the ratio was substantially smaller and falls within a physiologically plausible range
425 for alpha-band oscillations ($< 4:1$). Overall artifact suppression appeared to be slightly worse
426 during block 3 as compared to block 2.

427 The event-related envelope of the sham group was consistent with the pattern of alpha-power
428 decrease typically observed after stimulus onset in the MR task in both sensor types. This was
429 confirmed by the permutation cluster analysis, which revealed significant positive clusters in
430 the magnetometer and the gradiometer data ($p_{cluster} < .001$, **Figure 6A,C**; significant sensors
431 are marked by black dots), and further supported by the high correlation between source-level
432 power modulation and envelope difference of magnetometer ($r = .96$, $t_8 = 10.17$, $p < .001$,
433 **Figure 6B**) and gradiometer channels ($r = .88$, $t_8 = 5.23$, $p < .001$; **Figure 6D**). In the stimulation
434 group, time-course and topography of the envelope overall exhibited the opposite pattern with
435 lower amplitudes before stimulus onset and increased amplitude thereafter. In addition, the
436 envelope time-course of gradiometers shows a prominent rhythmic activity in the range of 1 to
437 2 Hz. This could potentially reflect heart-beat related modulations of the tACS waveform (Noury
438 et al., 2016). However, given that this rhythmic activity was only observed in one sensor type
439 and in a relatively systematic manner, it more likely reflects a technical artifact. Importantly, no
440 such rhythmic modulation was evident in the time-frequency representations after LCMV (**Fig-**
441 **ure 4**). Results of the cluster analysis revealed positive clusters in the gradiometer data in only
442 a few frontal sensors ($p_{cluster} < .05$, **Figure 6**, top left) as well as positive and negative clusters
443 for some magnetometer channels ($p_{cluster} < .05$). No significant correlation was evident between
444 the observed source-level power modulations and the sensor-level envelope differences in
445 magnetometer ($r = .13$, $t_8 = 0.37$, $p = .72$) or gradiometer sensors ($r = .26$, $t_8 = 0.75$, $p = .47$).
446 Overall, results do not support the idea that the effects observed on the source-level can be
447 explained by systematic, task-related changes in artifact strength. Very few channels were
448 found to exhibit significant, task-related power modulations. Those that did, rather seemed so
449 show a reversed pattern of artifact modulation as compared to the source-level data.

450 **4 Discussion**

451 To date, only few studies have investigated the effects of tACS on oscillatory activity in the
452 human brain *during* stimulation (Helfrich et al., 2014; Voss et al., 2014; Ruhnau et al., 2016),
453 due to the massive electromagnetic artifact encountered during the measurement. The current
454 study adds to this line of research by characterizing how event-related oscillatory activity, dur-
455 ing a cognitive task, reacts to externally applied perturbations in the same frequency band.
456 Theoretically, tACS could counteract, overwrite or enhance the oscillations underlying perfor-
457 mance of the task.

458 Results show that, rather than counteracting or overwriting the event-related down-regulation
459 of oscillatory power during the mental rotation (MR) task, continuous application of tACS facil-
460 itated the pre-existing difference between pre- and post-stimulus power in the alpha-band. This
461 finding indicates that tACS exerts its effects differently during pre- and post-stimulus intervals.
462 Given that tACS is usually observed to facilitate power of the targeted brain oscillation after
463 stimulation, the current finding seems most likely to be caused by stronger enhancement of
464 alpha-power prior to stimulus onset (Neuling et al., 2013; Veniero et al., 2015; Kasten and
465 Herrmann, 2017), rather than inhibition of post-stimulus alpha-power. Unfortunately, this can-
466 not be resolved using the current data, as the contrast between pre- and post-stimulus intervals
467 was necessary to account for residual tACS artifacts. To directly observe differential effects of
468 tACS on event-related brain oscillations, future work might make use of amplitude-modulated
469 tACS (AM-tACS), which has been proposed as a strategy to overcome the strong electrophys-
470 iological artifact in the range of the targeted brain oscillation (Witkowski et al., 2016). This new
471 stimulation waveform has very recently been shown to exhibit similar entrainment mechanisms
472 as conventional sine-wave tACS, in a computational model (Negahbani et al., 2018). However,
473 it should be noted that two recent studies cast doubts on whether AM-tACS is entirely free of
474 stimulation artifacts in the range of the targeted brain oscillation (Minami and Amano, 2017;
475 Kasten et al., 2018). Thus careful assessment of brain signals recorded during stimulation
476 would still be required.

477 A differential effect of tACS on pre- and post-stimulus intervals can be interpreted in terms of
478 a short-scale, state-dependency of tACS effects. Several studies have demonstrated that tACS
479 effects are state-dependent on larger time scales. On the one hand, tACS in the alpha-band
480 seems to only be effective when the targeted brain oscillation is comparatively low in ampli-
481 tude, e.g. during eyes open, but not during eyes closed (Neuling et al., 2013; Alagapan et al.,
482 2016; Ruhnau et al., 2016). On the other hand, an involvement of the targeted brain oscillation
483 in a given state (or task) also seems necessary to successfully induce tACS effects (Feurra et
484 al., 2013). In the simplest case, pre- and post-stimulus intervals in the current study reflect two
485 distinct brain states (a resting or preparatory state and a MR state), that differ in terms of alpha-
486 oscillation involvement and susceptibility to tACS. This pattern is in line with predictions derived
487 from synchronization theory, which require the presence of a self-sustained oscillator for en-
488 trainment to occur (Pikovsky et al., 2003). Consequently, tACS might exhibit its effect during
489 the pre- but not during the post-stimulus interval where alpha oscillations are suppressed due
490 to the task.

491 Although the current findings converge with observations of facilitated event-related desyn-
492 chronization (ERD) after tACS (Kasten and Herrmann, 2017), it is important to emphasize that
493 online effects of tACS (during stimulation) cannot directly be inferred from effects measured
494 after stimulation. While computational models and animal experiments suggest entrainment as
495 the core mechanism of online tACS effects (Fröhlich and McCormick, 2010; Ozen et al., 2010;
496 Reato et al., 2010), there is increasing evidence that the aftereffects of tACS might be better
497 explained by mechanisms of neural plasticity (Zaehle et al., 2010; Vossen et al., 2015). Differ-
498 ent mechanisms of action, during and after stimulation, could in principle lead to different ef-
499 fects of tACS on event-related oscillations. Thus, direct observations of tACS online effects
500 are inevitable to predict and understand behavioral outcomes of tACS experiments.

501 The observed enhancement of event-related alpha-power modulation can explain previous
502 results of better performance in the MR task during tACS (Kasten and Herrmann, 2017). Men-
503 tal rotation tasks typically feature alpha oscillations prior to stimulus onset, followed by task
504 induced suppression of the oscillation. The suppression typically lasts until participants finish

505 task execution (Michel et al., 1994). Studies using repetitive transcranial magnetic stimulation
506 (rTMS) and neurofeedback training (NFT) have demonstrated facilitated MR performance
507 when targeting spontaneous alpha oscillations during the pre-stimulus interval (Klimesch et
508 al., 2003; Hanslmayr et al., 2005; Zoefel et al., 2011). More broadly, alpha oscillations have
509 been suggested to enhance performance, in a variety of tasks, by suppressing activity in task
510 irrelevant areas of the brain or in preparation for an upcoming event, which has been referred
511 to as 'gating by inhibition' (Jensen and Mazaheri, 2010). By selectively enhancing pre-stimulus
512 alpha-power, tACS could facilitate the preparatory gating and thus benefit subsequent task
513 performance.

514 While the results are in agreement with previous findings (Kasten and Herrmann, 2017), they
515 contradict observations of Neuling et al. (2015). That study reported a tendency for reduced
516 alpha desynchronization elicited by a passive visual task during tACS. However, the authors
517 calculated relative change (computed similar to ERD/ERS) to capture event-related alpha
518 desynchronization, which is vulnerable to residual artifacts in the data. As shown in **Equation**
519 **2 and 3**, such a residual artifact would lead to a biased (larger) denominator, resulting in sys-
520 tematic underestimations of event-related desynchronization (ERD), within the stimulated fre-
521 quency band. Using the absolute power difference (here termed $ER\Delta_{Pow}$), between two time
522 intervals within the same stimulation condition (i.e. pre-/post-stimulus alpha-power), appears
523 to be a more robust measure to capture online effects of tACS. Using such a procedure, the
524 residual artifact cancels out during the subtraction process. Importantly, this cancelation as-
525 sumes that the strength of the residual artifact is relatively stable between conditions and un-
526 correlated with the task. Such systematic modulations could in principle occur if the task elicits
527 systematic changes in physiological processes like heart-beat, respiration, or skin conduct-
528 ance (Noury et al., 2016). While there was no evidence for such a systematic change in artifact
529 strength that could explain the observed pattern in the current data, the possibility has to be
530 taken into account when using stimuli that can elicit stronger physiological responses (e.g.
531 emotional pictures or demanding motor tasks). However, the impact of these modulations on

532 the artifact suppression, as compared to the size of the physiological effect on the brain, has
533 not been thoroughly characterized yet.

534 In addition to the observed effect of tACS on power modulations in the alpha-band, the data
535 revealed a trend towards increased event-related power modulations in the lower beta-band
536 during tACS. This observation could be indicative of a rather unspecific effect of tACS (Kleinert
537 et al., 2017). Alternatively, the effect in the lower beta-band could be explained by entrainment
538 or as a resonance phenomenon at the first harmonic of subjects' stimulation frequency
539 (Herrmann, 2001; Herrmann et al., 2016a). Further, cross-frequency interactions between al-
540 pha and beta oscillations (Palva et al., 2005) could underlie the effects, resulting in co-modu-
541 lation of beta oscillations stemming from tACS effects in the alpha-band.

542 Contradicting with the previous finding of a prolonged, tACS-induced ERD increase in the al-
543 pha-band (Kasten and Herrmann, 2017) and despite the substantial online effects, only a
544 short-lasting aftereffect during the first block after stimulation was observed, if at all. Several
545 studies have successfully shown persistent effects of tACS on alpha-power during rest (i.e.
546 Kasten et al., 2016; Neuling et al., 2013; Veniero et al., 2015; Vossen et al., 2015). A possible
547 explanation for the lack of a sustained tACS effect, in the current study, was the relatively low
548 stimulation intensity as compared to the aforementioned experiments.

549 Similar to previous work (Kasten and Herrmann, 2017), a significantly stronger increase in MR
550 performance was observed in the stimulation group as compared to the sham group. Unfortu-
551 nately, it cannot be ruled out that this effect might have been partly driven by differences in
552 baseline performance between the two groups. This could also explain the absence of previ-
553 ously observed correlations between performance increase and facilitated alpha-power mod-
554 ulation (Kasten and Herrmann, 2017), which would have further supported the physiological
555 findings. Alternatively, the strong effect of tACS on participants' alpha-power modulation during
556 stimulation might have caused ceiling effects such that, beyond a certain level, MR perfor-
557 mance could not be facilitated any further. However, due to the differences in baseline perfor-
558 mance, interpretability of the current behavioral results is limited. Nonetheless, this does not
559 contradict the physiological effects, which were the main focus of the current study. MR tasks

560 induce comparably long-lasting event-related power modulations (Michel et al., 1994); a ben-
561 efcial property when studying tACS effects on event-related oscillations. In the current exper-
562 iment, this came at the cost of overall high task performance in both groups. Future studies
563 might therefore benefit from more difficult MR paradigms (e.g. only including large rotation
564 angles).

565 In addition to investigating the concurrent effects of tACS on event-related oscillations, the
566 current study made an attempt to quantify the artifact suppression capabilities of LCMV beam-
567 forming. To this end, the oscillatory power around the stimulated frequency during tACS, was
568 compared to an artifact-free estimate of participants' natural brain signal (alpha-power). This
569 allowed to estimate the magnitude of the stimulation artifact relative to the brain signal of in-
570 terest before and after artifact suppression. In the current study, this artifact-to-brain-signal-
571 ratio was reduced from greater than 2,500,000:1, before LCMV, to ~3:1 thereafter, with
572 stronger artifacts around stimulation electrodes and cables (~10:1). Since the power values
573 obtained during stimulation will always contain a mixture of residual tACS artifact and brain
574 signal, this ratio can only provide an upper boundary for the size of the residual artifact. Alpha-
575 power increase, by a factor of 3 or 4, fall into a physiologically plausible range for spontaneous
576 of stimulation-induced alpha-power changes, consistent with previous work on tACS afteref-
577 fects (Neuling et al., 2013; Kasten and Herrmann, 2017; Stecher et al., 2017). The artifact-to-
578 brain-signal-ratio might nevertheless be a useful tool for future studies to assess whether a
579 residual artifact falls within the same order of magnitude as the brain signal of interest. It might
580 also be used to evaluate and optimize the performance of artifact suppression techniques, i.e.
581 by tuning relevant parameters. Thus far, artifact suppression approaches have mostly been
582 evaluated subjectively, i.e. by inspecting raw time series, (time-) frequency-spectra or ERPs
583 (Helfrich et al., 2014; Neuling et al., 2015; Witkowski et al., 2016). The artifact-to-brain-signal-
584 ratio provides a more objective evaluation of the artifact size, relative to the brain signal of
585 interest, and is scale-free, allowing for easy comparison of different artifact suppression ap-

586 proaches even between different measurement modalities (EEG/MEG, LCMV, template sub-
587 traction etc.). In addition, the mapping of residual artifact strength allows the assessment of
588 overlap between ‘hot spots’ of residual artifacts and regions of interest.

589 The findings presented in the current study provide the first direct insights concerning the
590 online effects of tACS on event-related oscillations in humans. The effects were investigated
591 using a rather simplistic approach, utilizing only two conditions (stimulation vs. sham) and one
592 stimulation frequency, targeting posterior alpha oscillations with a Cz-Oz montage. This path
593 was chosen to establish an analysis framework, including controls, for the investigation of con-
594 current effects of tACS. Success at this stage would greatly facilitate approaches with more
595 complex designs, requiring larger sample sizes and higher computational efforts. TACS exper-
596 iments generally allow for a multitude of control and contrast conditions, including alternative
597 electrode montages and frequencies. The current study can therefore neither resolve fre-
598 quency nor montage specificity of tACS effects. However, with the present results and the
599 proposed analysis pipeline, the current study paves the way for further investigations of mon-
600 tage and frequency specificity of tACS effects, specifically on event-related oscillatory dynam-
601 ics during various cognitive tasks.

602 **5 Author contributions**

603 FHK, BM and CSH conceived the study and wrote the manuscript. FHK and BM collected the
604 data. FHK analyzed the data. BM and CSH provided equipment and funding for the study.

605 **6 References**

606 Alagapan S, Schmidt SL, Lefebvre J, Hadar E, Shin HW, Fröhlich F (2016) Modulation of
607 Cortical Oscillations by Low-Frequency Direct Cortical Stimulation Is State-Dependent.
608 PLOS Biol 14:e1002424.

609 Alekseichuk I, Diers K, Paulus W, Antal A (2016) Transcranial electrical stimulation of the
610 occipital cortex during visual perception modifies the magnitude of BOLD activity: A
611 combined tES–fMRI approach. Neuroimage 140:110–117.

- 612 Ali MM, Sellers KK, Frohlich F (2013) Transcranial Alternating Current Stimulation Modulates
613 Large-Scale Cortical Network Activity by Network Resonance. *J Neurosci* 33:11262–
614 11275.
- 615 Basar E, Basar-Eroglu C, Karakas S, Schürmann M (2000) Brain oscillations in perception and
616 memory. *Int J Psychophysiol* 35:95–124.
- 617 Brunoni AR, Amadera J, Berbel B, Volz MS, Rizzerio BG, Fregni F (2011) A systematic review
618 on reporting and assessment of adverse effects associated with transcranial direct current
619 stimulation. *Int J Neuropsychopharmacol* 14:1133–1145.
- 620 Buzsáki G (2006) *Rhythms of the Brain*. Oxford University Press.
- 621 Cabral-Calderin Y, Williams KA, Opitz A, Dechent P, Wilke M (2016) Transcranial alternating
622 current stimulation modulates spontaneous low frequency fluctuations as measured with
623 fMRI. *Neuroimage* 141:88–107.
- 624 Feurra M, Pasqualetti P, Bianco G, Santarnecchi E, Rossi A, Rossi S (2013) State-dependent
625 effects of transcranial oscillatory currents on the motor system: what you think matters. *J*
626 *Neurosci* 33:17483–17489.
- 627 Fröhlich F, McCormick DA (2010) Endogenous Electric Fields May Guide Neocortical Network
628 Activity. *Neuron* 67:129–143.
- 629 Ganis G, Kievit R (2015) A New Set of Three-Dimensional Shapes for Investigating Mental
630 Rotation Processes: Validation Data and Stimulus Set. *J Open Psychol Data* 3.
- 631 Hanslmayr S, Sauseng P, Doppelmayr M, Schabus M, Klimesch W (2005) Increasing
632 Individual Upper Alpha Power by Neurofeedback Improves Cognitive Performance in
633 Human Subjects. *Appl Psychophysiol Biofeedback* 30:1–10.
- 634 Helfrich RF, Schneider TR, Rach S, Trautmann-Lengsfeld SA, Engel AK, Herrmann CS (2014)
635 Entrainment of Brain Oscillations by Transcranial Alternating Current Stimulation. *Curr*
636 *Biol* 24:333–339.

- 637 Herrmann CS (2001) Human EEG responses to 1-100 Hz flicker: resonance phenomena in
638 visual cortex and their potential correlation to cognitive phenomena. *Exp brain Res*
639 137:346–353.
- 640 Herrmann CS, Murray MM, Ionta S, Hutt A, Lefebvre J (2016a) Shaping Intrinsic Neural
641 Oscillations with Periodic Stimulation. *J Neurosci* 36:5328–5337.
- 642 Herrmann CS, Strüber D, Helfrich RF, Engel AK (2016b) EEG oscillations: From correlation to
643 causality. *Int J Psychophysiol* 103:12–21.
- 644 Jensen O, Mazaheri A (2010) Shaping functional architecture by oscillatory alpha activity:
645 gating by inhibition. *Front Hum Neurosci* 4:186.
- 646 Kar K, Duijnhouwer J, Krekelberg B (2017) Transcranial Alternating Current Stimulation
647 Attenuates Neuronal Adaptation. *J Neurosci* 37:2325–2335.
- 648 Kar K, Krekelberg B (2014) Transcranial Alternating Current Stimulation Attenuates Visual
649 Motion Adaptation. *J Neurosci* 34:7334–7340.
- 650 Kasten FH, Dowsett J, Herrmann CS (2016) Sustained Aftereffect of α -tACS Lasts Up to 70
651 min after Stimulation. *Front Hum Neurosci* 10:1–9.
- 652 Kasten FH, Herrmann CS (2017) Transcranial Alternating Current Stimulation (tACS)
653 Enhances Mental Rotation Performance during and after Stimulation. *Front Hum*
654 *Neurosci* 11:1–16.
- 655 Kasten FH, Negahbani E, Fröhlich F, Herrmann CS (2018) Non-linear transfer characteristics
656 of stimulation and recording hardware account for spurious low-frequency artifacts during
657 amplitude modulated transcranial alternating current stimulation (AM-tACS). *Neuroimage*
658 (in press).
- 659 Kleiner M, Brainard DH, Pelli DG, Broussard C, Wolf T, Niehorster D (2007) What's new in
660 Psychtoolbox-3? *Perception* 36:S14.
- 661 Kleinert M-L, Szymanski C, Müller V (2017) Frequency-Unspecific Effects of θ -tACS Related

Kasten et al., 2018 Facilitated event-related power-modulations during tACS

- 662 to a Visuospatial Working Memory Task. *Front Hum Neurosci* 11:1–16.
- 663 Klimesch W (1999) EEG alpha and theta oscillations reflect cognitive and memory
664 performance: A review and analysis. *Brain Res Rev* 29:169–195.
- 665 Klimesch W, Sauseng P, Gerloff C (2003) Enhancing cognitive performance with repetitive
666 transcranial magnetic stimulation at human individual alpha frequency. *Eur J Neurosci*
667 17:1129–1133.
- 668 Klimesch W, Sauseng P, Hanslmayr S (2007) EEG alpha oscillations: The inhibition-timing
669 hypothesis. *Brain Res Rev* 53:63–88.
- 670 Lustenberger C, Boyle MR, Foulser AA, Mellin JM, Fröhlich F (2015) Functional role of frontal
671 alpha oscillations in creativity. *Cortex* 67:74–82.
- 672 Mäkelä N, Sarvas J, Ilmoniemi RJ (2017) Proceedings #17. A simple reason why beamformer
673 may (not) remove the tACS-induced artifact in MEG. *Brain Stimul* 10:e66–e67.
- 674 Marshall L, Helgadóttir H, Mölle M, Born J (2006) Boosting slow oscillations during sleep
675 potentiates memory. *Nature* 444:610–613.
- 676 Michel CM, Kaufman L, Williamson SJ (1994) Duration of EEG and MEG α Suppression
677 Increases with Angle in a Mental Rotation Task. *J Cogn Neurosci* 6:139–150.
- 678 Minami S, Amano K (2017) Illusory Jitter Perceived at the Frequency of Alpha Oscillations.
679 *Curr Biol* 27:2344–2351.e4.
- 680 Negahbani E, Kasten FH, Herrmann CS, Fröhlich F, Frohlich F (2018) Targeting alpha-band
681 oscillations in a cortical model with amplitude-modulated high-frequency transcranial
682 electric stimulation. *Neuroimage* 173:3–12.
- 683 Neuling T, Rach S, Herrmann CS (2013) Orchestrating neuronal networks: sustained after-
684 effects of transcranial alternating current stimulation depend upon brain states. *Front Hum*
685 *Neurosci* 7:161.
- 686 Neuling T, Ruhnau P, Fusca M, Demarchi G, Herrmann CS, Weisz N (2015) Friends, not foes:

- Kasten et al., 2018 Facilitated event-related power-modulations during tACS
712 desynchronization: Basic principles. *Clin Neurophysiol* 110:1842–1857.
- 713 Pikovsky A, Rosenblum M, Kurths J (2003) *Synchronization: A Universal Concept in Nonlinear*
714 *Sciences*. Cambridge: Cambridge University Press.
- 715 Reato D, Rahman A, Bikson M, Parra LC (2010) Low-Intensity Electrical Stimulation Affects
716 Network Dynamics by Modulating Population Rate and Spike Timing. *J Neurosci*
717 30:15067–15079.
- 718 Ruhnau P, Neuling T, Fuscá M, Herrmann CS, Demarchi G, Weisz N (2016) Eyes wide shut:
719 Transcranial alternating current stimulation drives alpha rhythm in a state dependent
720 manner. *Sci Rep* 6:27138.
- 721 Shepard RN, Metzler J (1971) Mental rotation of three-dimensional objects. *Science* 171:701–
722 703.
- 723 Soekadar SR, Witkowski M, Cossio EG, Birbaumer N, Robinson SE, Cohen LG (2013) In vivo
724 assessment of human brain oscillations during application of transcranial electric
725 currents. *Nat Commun* 4:2032.
- 726 Stecher HI, Pollok TM, Strüber D, Sobotka F, Herrmann CS, Christoph S (2017) Ten Minutes
727 of α -tACS and Ambient Illumination Independently Modulate EEG α -Power. *Front Hum*
728 *Neurosci* 11:1–10.
- 729 Taulu S, Simola J, Kajola M (2005) Applications of the signal space separation method. *IEEE*
730 *Trans Signal Process* 53:3359–3372.
- 731 Van Veen BD, Van Drongelen W, Yuchtman M, Suzuki A (1997) Localization of brain electrical
732 activity via linearly constrained minimum variance spatial filtering. *IEEE Trans Biomed*
733 *Eng* 44:867–880.
- 734 Veniero D, Vossen A, Gross J, Thut G (2015) Lasting EEG/MEG Aftereffects of Rhythmic
735 Transcranial Brain Stimulation: Level of Control Over Oscillatory Network Activity. *Front*
736 *Cell Neurosci* 9:477.

- Kasten et al., 2018 Facilitated event-related power-modulations during tACS
- 737 Violante IR, Li LM, Carmichael DW, Lorenz R, Leech R, Hampshire A, Rothwell JC, Sharp DJ
738 (2017) Externally induced frontoparietal synchronization modulates network dynamics
739 and enhances working memory performance. *Elife* 6.
- 740 Voss U, Holzmann R, Hobson A, Paulus W, Koppehele-Gossel J, Klimke A, Nitsche M a (2014)
741 Induction of self awareness in dreams through frontal low current stimulation of gamma
742 activity. *Nat Neurosci* 17:810–812.
- 743 Vossen A, Gross J, Thut G (2015) Alpha Power Increase After Transcranial Alternating Current
744 Stimulation at Alpha Frequency (α -tACS) Reflects Plastic Changes Rather Than
745 Entrainment. *Brain Stimul* 8:499–508.
- 746 Vosskuhl J, Huster RJ, Herrmann CS (2016) BOLD signal effects of transcranial alternating
747 current stimulation (tACS) in the alpha range: A concurrent tACS–fMRI study.
748 *Neuroimage* 140:118–125.
- 749 Wach C, Krause V, Moliadze V, Paulus W, Schnitzler A, Pollok B (2013) Effects of 10Hz and
750 20Hz transcranial alternating current stimulation (tACS) on motor functions and motor
751 cortical excitability. *Behav Brain Res* 241:1–6.
- 752 Witkowski M, Garcia-Cossio E, Chander BS, Braun C, Birbaumer N, Robinson SE, Soekadar
753 SR (2016) Mapping entrained brain oscillations during transcranial alternating current
754 stimulation (tACS). *Neuroimage* 140:89–98.
- 755 Zaehle T, Rach S, Herrmann CS (2010) Transcranial Alternating Current Stimulation
756 Enhances Individual Alpha Activity in Human EEG. *PLoS One* 5:13766.
- 757 Zoefel B, Huster RJ, Herrmann CS (2011) Neurofeedback training of the upper alpha
758 frequency band in EEG improves cognitive performance. *Neuroimage* 54:1427–1431.
- 759

760 **7 Figure captions**

761 **Figure 1: Experimental Procedures. (A)** Time course of the experiment. Blue indicates peri-
762 ods during which the MR task was performed, grey indicates intermittent resting periods. **(B)**
763 Positions of stimulation electrodes (red/blue) and layout of MEG sensors (yellow/green). Stim-
764 ulation electrodes were placed centered above Cz (7 x 5 cm) and Oz (4 x 4 cm) of the interna-
765 tional 10-10 system. MEG was recorded from 102 locations. Each location contains a sensor
766 triplet of one magnetometer and two orthogonal planar gradiometers, resulting in a total of 306
767 channels. Sensor locations used to determine participants' individual alpha frequency are
768 marked green. **(C)** Mental rotation task. Each trial started with the presentation of a white fixa-
769 tion cross at the center of the screen. After 3000 ms a mental rotation stimulus (two objects)
770 was presented and remained on screen for another 7000 ms. During this time participants
771 were required to judge whether the two objects presented were either different (example de-
772 picted in 2nd display) or identical (but rotated; 4th display). **A** and **C** are adapted from Kasten
773 and Herrmann (2017).

774

775 **Figure 2: Behavioral results. (A)** Change in task performance for *stimulation* and *sham*
776 group, relative to baseline, pooled over all experimental blocks. Boxes indicate the 25th and
777 75th percentile of the sample distribution (interquartile length), lines inside the boxes mark the
778 median. Whiskers extend to the most extreme values within 1.5 times the interquartile length.
779 Asterisks code for significance (* < .05). **(B)** Change in task performance relative to baseline
780 for *stimulation* and *sham* group depicted over experimental blocks. The grey area indicates
781 blocks that were performed during tACS or sham stimulation. **(C)** Change in RT for *stimulation*
782 and *sham* group relative to baseline pooled over experimental blocks. **(D)** Change in RT for
783 *stimulation* and *sham* group relative to baseline depicted over experimental blocks. Grey area
784 indicates blocks that were performed during tACS or sham stimulation.

785

786 **Figure 3: Event-related alpha-power modulation. (A)** Region of interest (ROI). Significant
787 cluster (pre- vs. post-stimulus power) in the IAF-band during the first block prior to tACS or

788 sham stimulation, computed over the whole sample ($p_{cluster} < .001$). Topographies depict t-
789 values mapped on an MNI standard surface. Statistical maps are thresholded at $\alpha < .01$. The
790 depicted cluster (blue) was used as ROI to extract the time course of alpha-power modulation,
791 relative to baseline, over blocks from the virtual channels. **(B)** Relative alpha-power modulation
792 within ROI depicted for each block. The grey area indicates blocks during tACS or sham stim-
793 ulation. Shaded areas represent standard error of the mean (*S.E.M.*). Dashed line depicts
794 baseline level. **(C)** Relative alpha-power modulation during tACS or sham (online) and after
795 stimulation (offline). Error bars represent *S.E.M.*, asterisks code for significant differences ($* <$
796 $.05$). **(D)** Relative alpha-power modulation during stimulation correlated with stimulation inten-
797 sity. Each point represents a single subjects' stimulation amplitude, and relative alpha-power
798 modulation, averaged over the two stimulation blocks (block 2 and 3). Please note that a stim-
799 ulation intensity was determined for all participants (including sham). However, only partici-
800 pants in the stimulation group had this intensity continuously applied during block 2 and 3 **(E)**
801 Relative power modulation in the lower beta-band (IAF + 3 Hz to IAF + 11 Hz) within the ROI
802 for each block. **(F)** Relative power modulation in the higher beta-band (IAF + 12 Hz to IAF +
803 20 Hz) within the ROI for each block. **(G+H)** Correlation between change in task performance
804 and relative alpha-power modulation during **(G)** and after tACS **(H)**. High, albeit non-significant
805 correlations were evident for the sham, but not the stimulation group.

806

807 **Figure 4: Normalized, baseline-subtracted TFRs and source topographies.** TFRs and
808 source topographies for *stimulation* (**Top Rows**) and *sham* group. (**Bottom Rows**). TFRs were
809 aligned at IAF and averaged over subjects in each group. The range from -2.5 to -0.5 prior to
810 stimulus onset (white bar) served as reference period for baseline subtraction. Spectra were
811 subsequently normalized by the power difference in the alpha-band (IAF \pm 2Hz) during the
812 baseline block (block 1) prior to stimulation. Normalization was performed such that the data
813 presented resemble data in the statistical analysis. Blocks 2 and 3 (dark grey) represent data
814 acquired during tACS or sham stimulation. All other blocks (light grey) were measured in ab-
815 sence of stimulation. Functional maps were averaged over subjects and projected onto an MNI

816 standard surface. Only activity within the analyzed ROI is depicted. A strong facilitation of
817 event-related power modulation around the IAF can be observed during tACS application
818 (block 2 and 3).

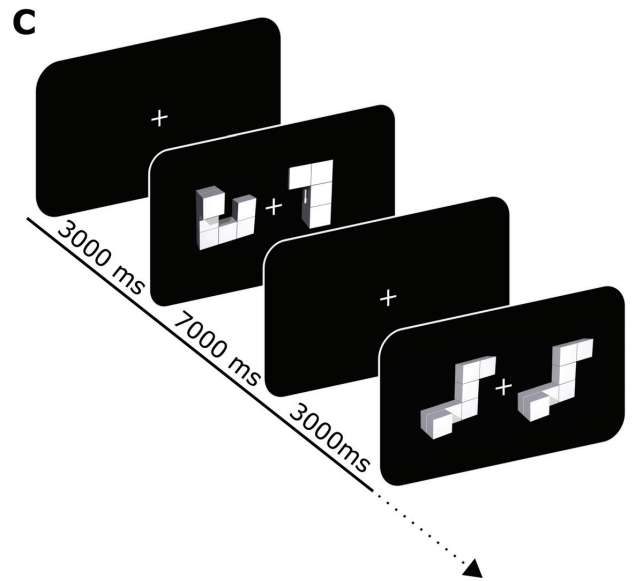
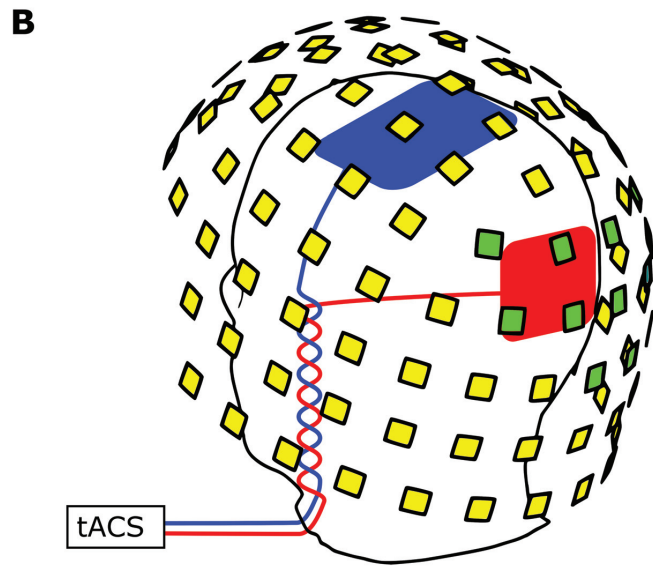
819

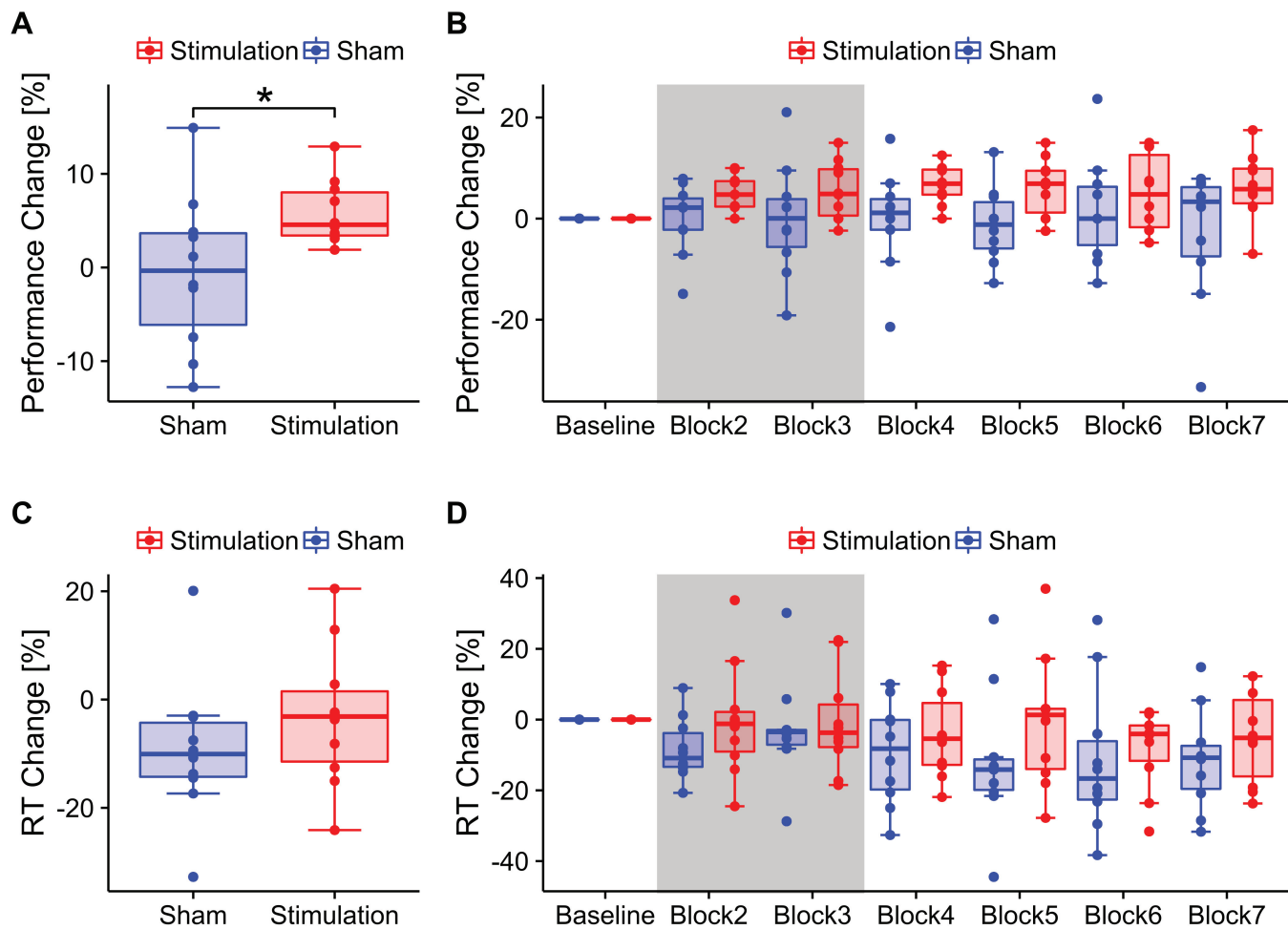
820 **Figure 5: Artifact-to-brain-signal topographies.** Topographies depict the average ratio be-
821 tween participants' pre-stimulus alpha-power, estimated during the baseline block, and resid-
822 ual artifact in the pre-stimulus interval during block 2 (**top row**) and 3 (**bottom row**). Results
823 are depicted only for the stimulation group. The ratio is strongest in central areas covered by
824 the stimulation electrodes and cables. Frontal and posterior areas within the ROI seem less
825 affected, with the ratio falling in a physiologically plausible range ($< 1:4$), such that residual
826 artifact and facilitatory effects of the stimulation or spontaneous increase of alpha-power can-
827 not be disentangled. Results have to be interpreted in terms of an upper boundary for the size
828 of the residual artifact, as each virtual channel contains a mixture of brain signal of interest and
829 artifact.

830

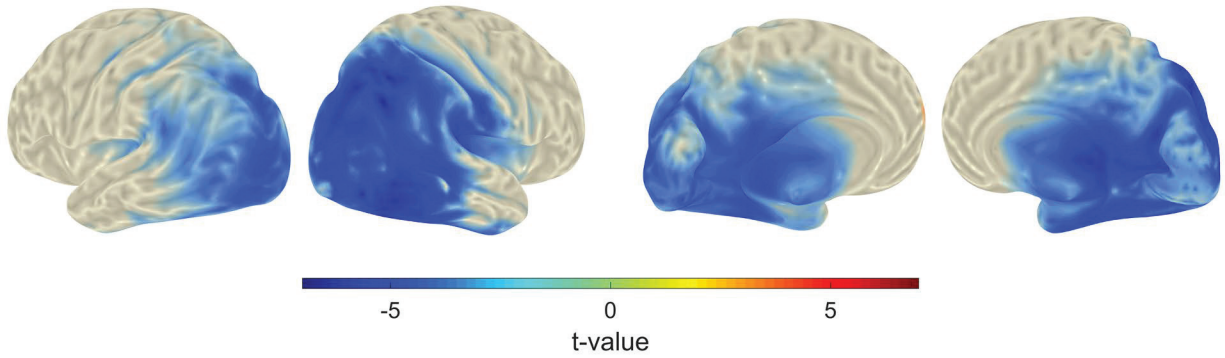
831 **Figure 6: Event-related artifact envelope. (A)** Topography and time course of the artifact
832 envelope around stimulus onset in gradiometer sensors. Topographies represent the ampli-
833 tude difference of the envelope, around the stimulation frequency between the reference (-2.5
834 to -0.5 sec) and the testing periods (0 to 2 sec). Darkened sensors mark locations in which this
835 difference was significant. Data of the sham group is depicted for comparison and reflects the
836 task-related modulation of endogenous alpha oscillations (visible shortly after stimulus onset,
837 vertical black bar at 0 sec) as no stimulation artifact was introduced to the data. Envelope
838 epochs of all subjects were demeaned before averaging to enhance comparability of the en-
839 velope modulation. Shaded areas depict standard error of the mean (*S.E.M.*). Gradiometer
840 time-courses were strongly dominated by rhythmic modulation around 1 Hz – 2 Hz that poten-
841 tially reflects a technical artifact in this sensor type. **(B)** Correlation between event-related mod-
842 ulation of the artifact envelope in gradiometer sensors and event-related alpha-power modu-
843 lation within the ROI after beamforming. The absence of a significant (or even moderately high)

844 correlation in the stimulation group provides supporting evidence that the effects observed in
845 source-space are not driven by systematic event-related modulations of tACS artifact strength.
846 **(C)** Topography and time course of the artifact envelope around stimulus onset in magnetom-
847 eter sensors. **(D)** Correlation between event-related modulation of the artifact envelope in mag-
848 netometers and alpha-power modulation within ROI after beamforming. Similar to the gradi-
849 ometer data, no correlation between source-level effects and artifact tACS artifact modulation
850 was observed.

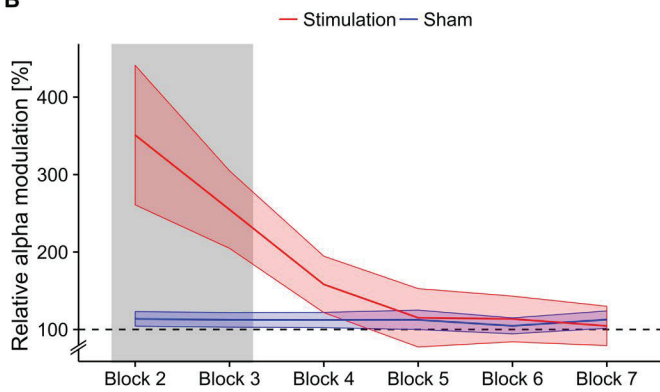




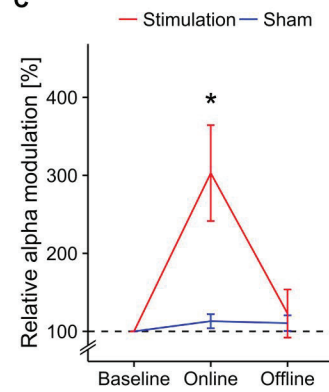
A



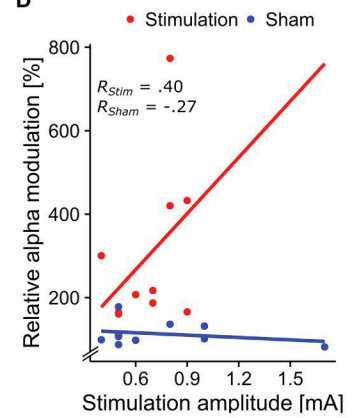
B



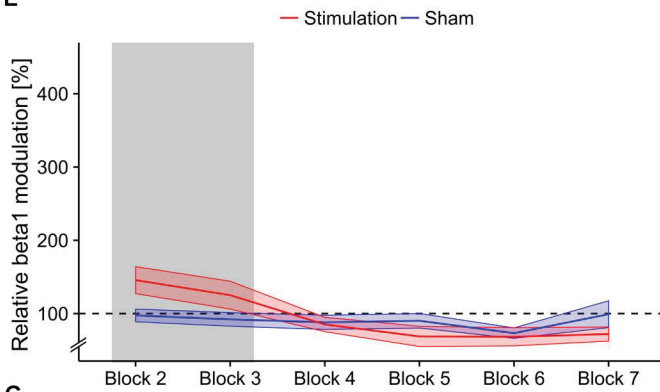
C



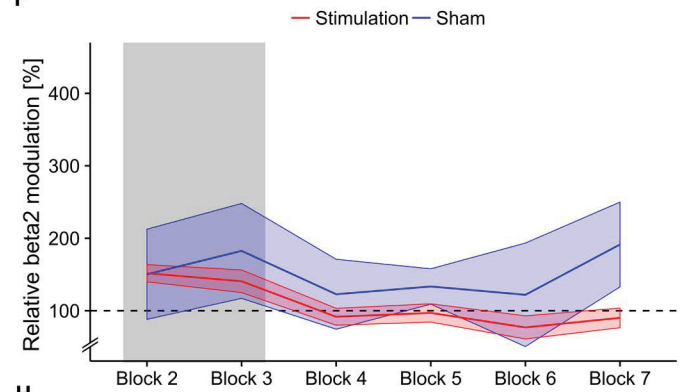
D



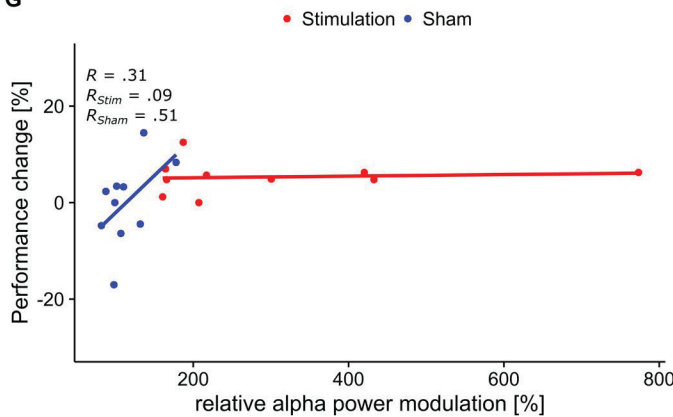
E



F



G



H

